Electronic Supplementary Information (ESI)

Directly Grown Co_3O_4 Nanowire Arrays on Ni-foam: Structural Effect of Carbon-free and Binder-free Cathodes for Li thium Oxygen Batteries

Hongkyung Lee[a]‡, Yun-Jung Kim[a]‡, Dong Jin Lee[a], Jongchan Song[a], Yong Min Lee[b], Hee-Tak Kim[a]** and Jung-Ki Park[a]*

[a]*Department of Chemical and Biomolecular Engineering, Korea Advanced Institute of Science and Technology, 291, Daehak-ro, Yuseong-gu, Daejeon 305-701, Republic of Korea*
[b]*Department of Applied Chemistry, Hanbat National University, Deokmyoung-dong, Yuseong-gu, Daejeon 305-719, Republic of Korea.*

* Corresponding author. Tel.: +82-42-350-3925; fax: +82-42-350-3910
E-mail: jungpark@kaist.ac.kr (J. –K. Park),
** Co-corresponding author. Tel.: +82-42-350-3916; fax: +82-42-350-3910
E-mail: heetak.kim@kaist.ac.kr (H. -T. Kim)

‡These authors have contributed equally to this work.

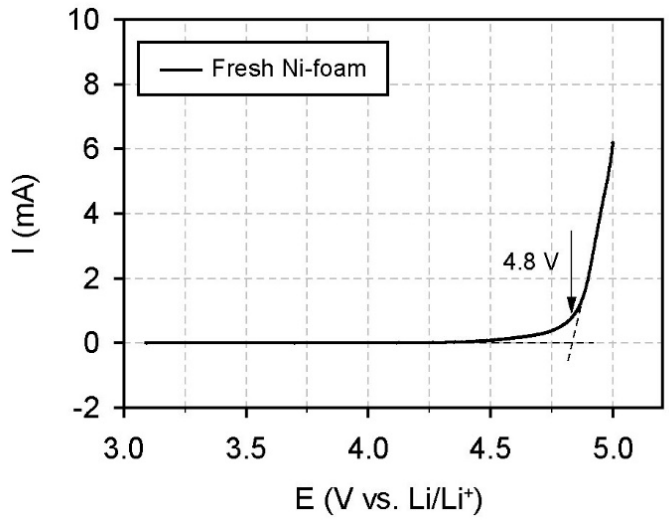

Fig. S1. Linear sweep voltammetry of the pristine Ni-foam in the DMSO electrolyte under O_2 atmosphere. (Scan rate: 0.5 mV s^{-1})

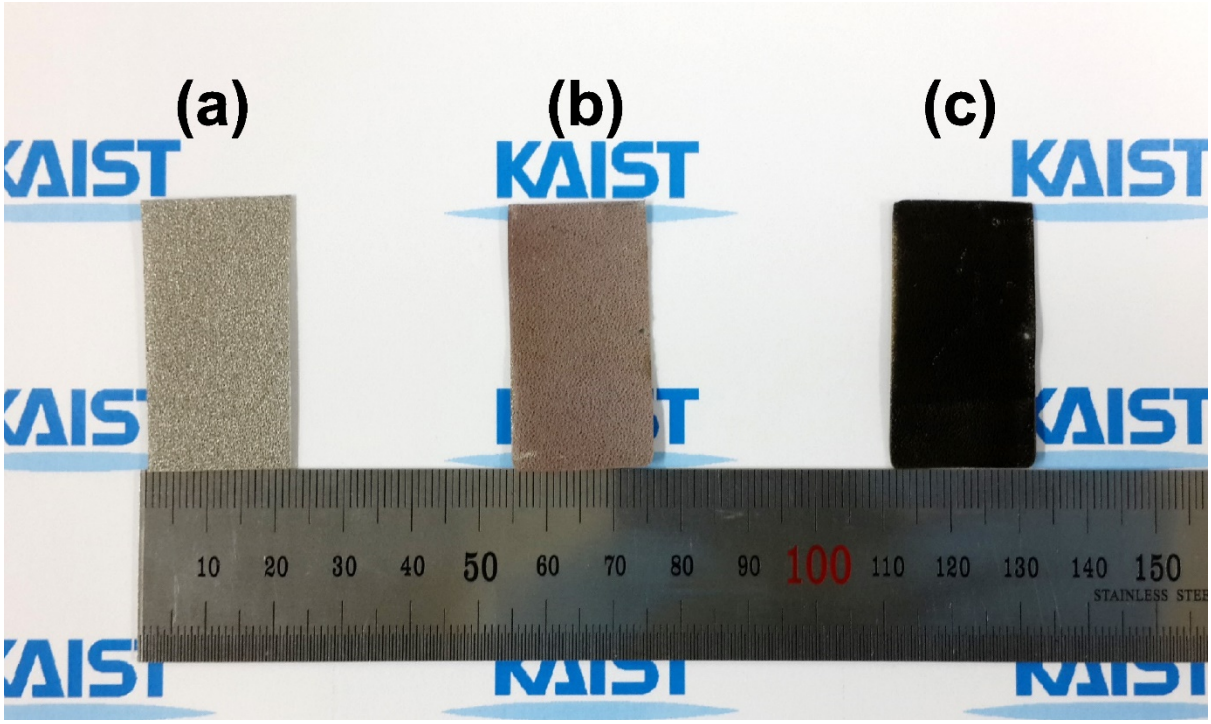

Fig. S2. Digital images of (a) pristine Ni-foam, (b) Ni-foam coated with pink precursors ($Co(OH)_{1.10}Cl_{0.2}(CO_3)_{0.35} \cdot 1.74H_2O$) on Ni-foam after a hydrothermal reaction, and (c) Co_3O_4 NW@Ni-foam converted by annealing in air at 250 ˚C for 1h

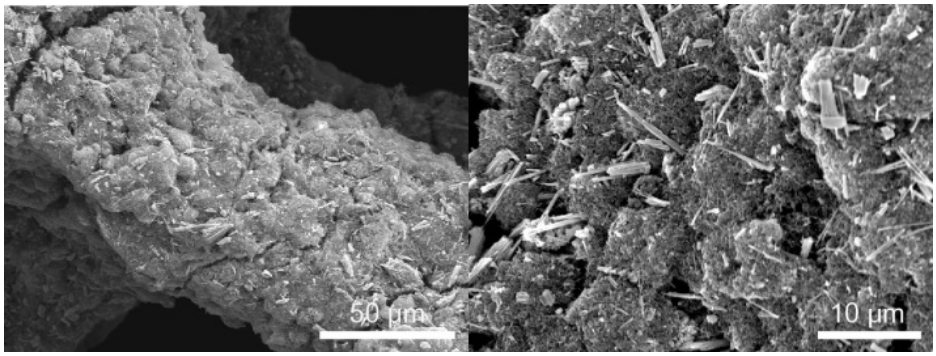

Fig. S3. SEM images of the surface of a Co_3O_4/KB/PTFE electrode prepared by a convention al slurry mixing method

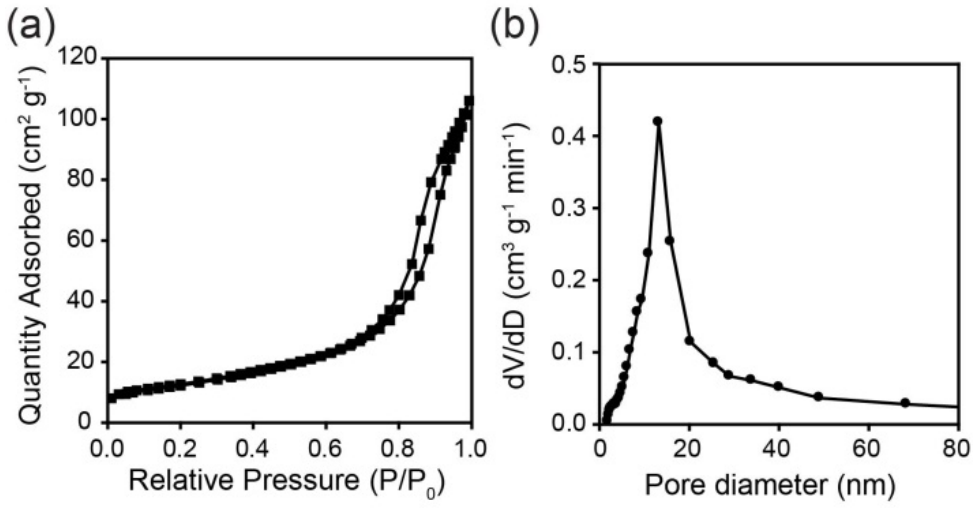

Fig. S4. (a) The N_2 gas adsorption-desorption isotherm loop, and (b) a histogram of the pore size distribution data for the Co_3O_4 NWs after a thermal treatment at 250℃

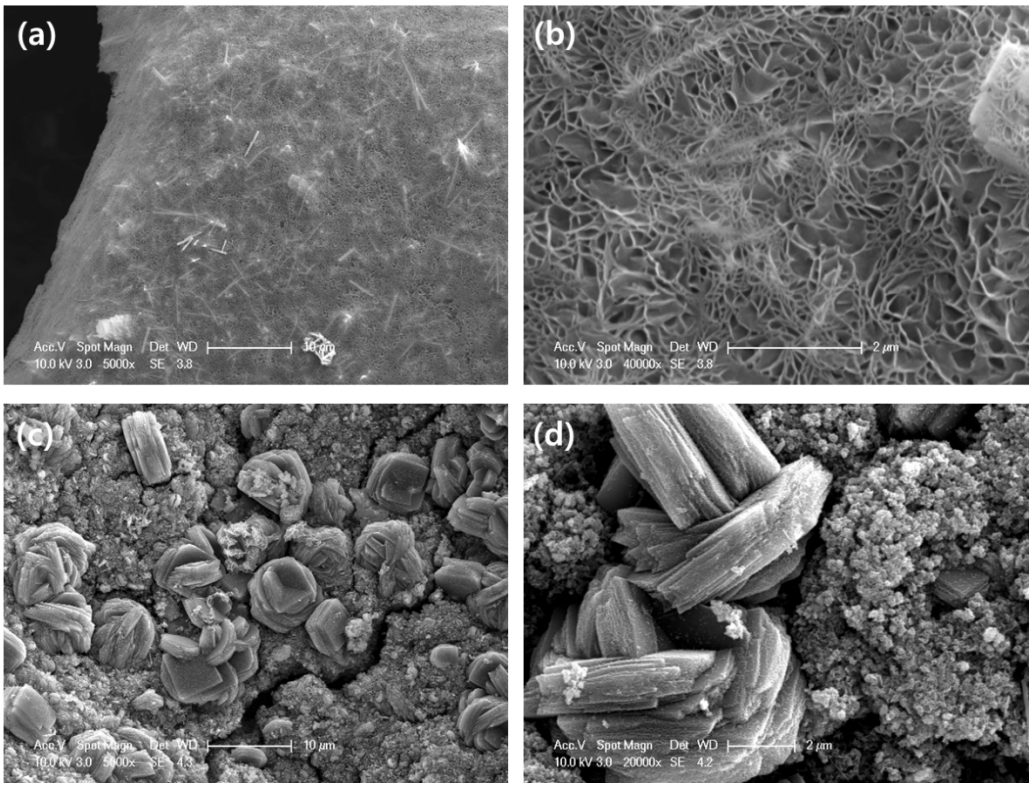

Fig. S5. SEM images of the Co_3O_4/KB/PTFE electrode ((a) 5000×, (b) 40000×) and the Co_3O_4/KB/PTFE electrode ((c) 5000×, (d) 20000×) taken after the first discharge to 2.25V.

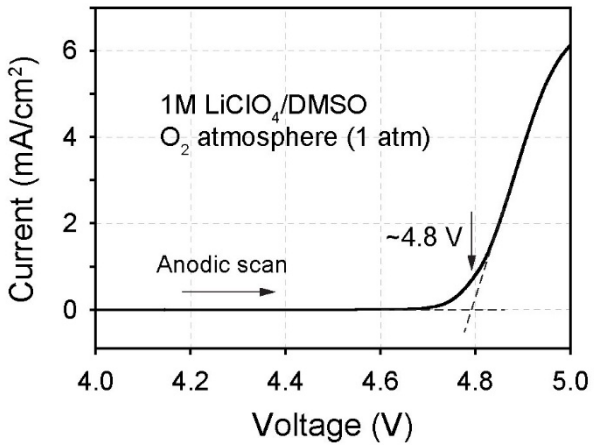

Fig. S6. Linear sweep voltammetry of a carbon paper electrode for investigating oxidative stability of the 1M $LiClO_4$/DMSO electrolyte under O_2 atmosphere (~1 atm) (scan rate: sweep rate of 0.1 mV s^{-1})

To avoid any interference from the oxidation of Li_2O_2, the carbon paper electrode which did not include any discharge products was used in this test.

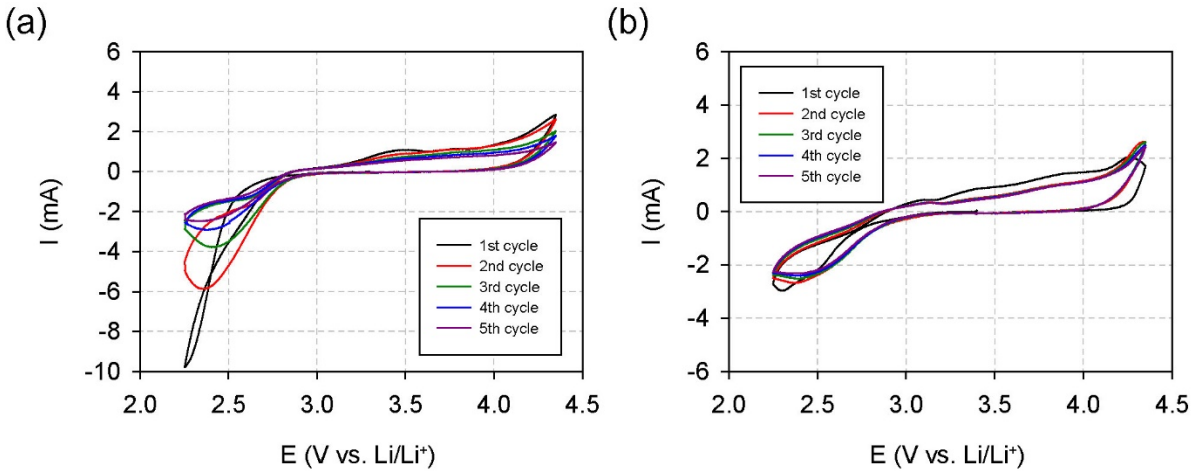

Fig. S7. Cyclic voltammetry of Li-O_2 cells with (a) Co_3O_4/KB/PTFE and (b) Co_3O_4 NW@Ni -foam electrodes during five cycles under O_2 atmosphere. The voltage range is 2.25 – 4.35 V vs. Li/Li^+ and a sweep rate is 0.5 mV s^{-1}.

As shown in Fig. S7, for the Co_3O_4/KB/PTFE electrode, while the first cathodic peak current was significantly high owing to large surface area of highly porous carbon, this peak current was rapidly diminished after the following cycles. Also the anodic current was also gradually decreased with the cycles. Because carbon and binder materials generate irreversible reaction products such as Li_2CO_3 and LiF, the peak currents for oxygen reduction and evolution reacti ons decrease as the irreversible products are accumulated and eventually deactivate the air ele ctrode. By contrast, for the Co_3O_4NW@Ni-foam, the oxidation and reduction currents were maintained over the cycles. This result indicates a reversibility in oxygen reduction and evolu tion reactions for the directly grown Co_3O_4 NWs.

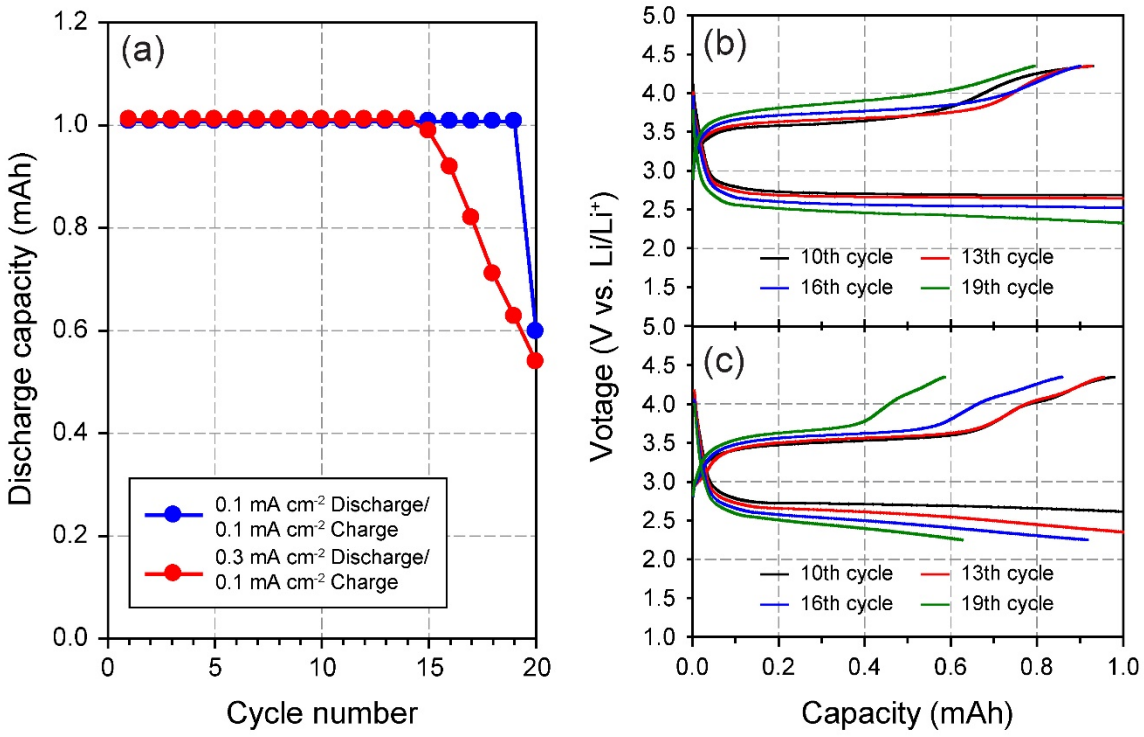

Fig. S8. (a) The curtailing cycle performance and discharge–charge profiles after 10 cycles of two cells discharged at (b) 0.1 and (c) 0.3 mA cm^{-2}, respectively, after which they were charged at the same charge rate of 0.1 mA cm^{-2}